Supplementary

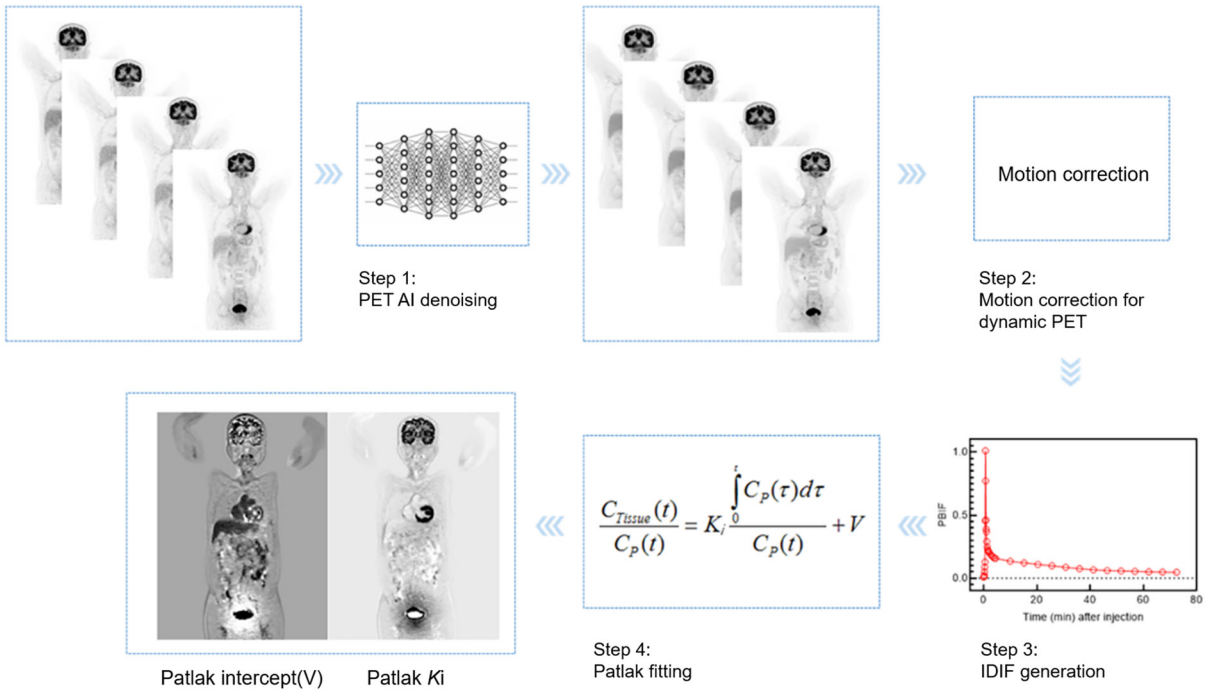

Figure S1 Patlak processing workflow. Four steps were used for Patlak processing, including deep learning-based denoising, automatic deformative motion correction of dynamic passes, generation of image-derived input function, and the Patlak fitting, after which the Patlak K_i images were obtained. AI, artificial intelligence; IDIF, image-derived input function; PET, positron emission tomography.

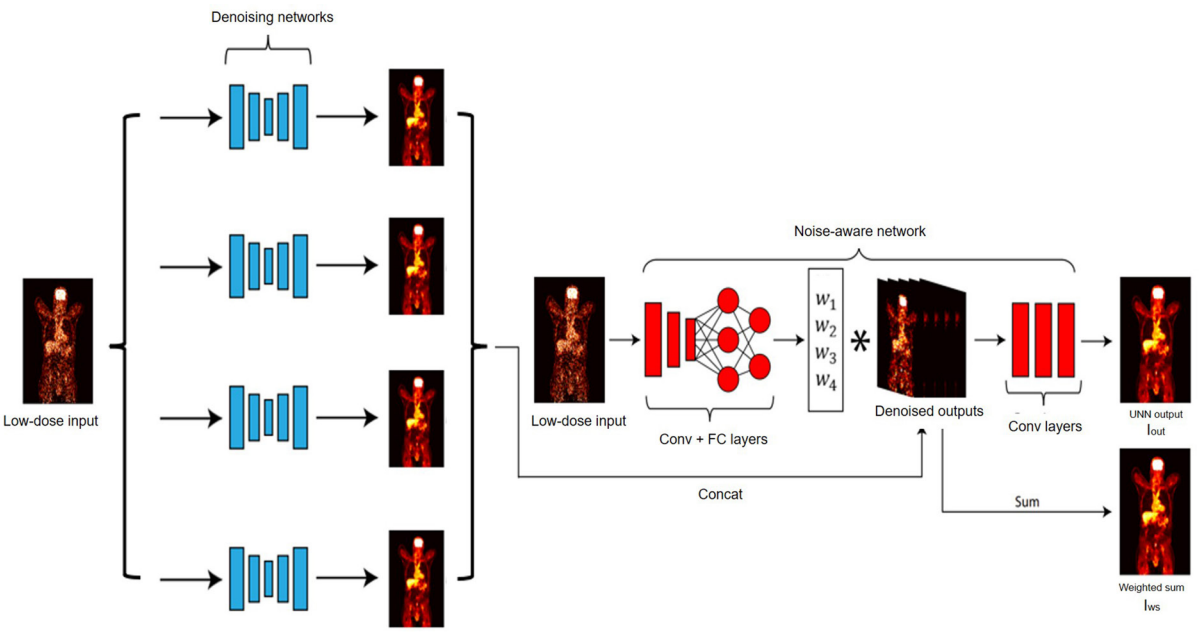

Figure S2 Framework of the modified UNN for FDG denoising. It consists of 4 noise levels of networks and 1 noise-aware network. w1 to w4 are 4 personalized weighting parameters that combine denoised outputs from 4 denoising networks. Conv, convolutional; FC, fully connected; FDG, fluorodeoxyglucose; UNN, Unified Noise-aware Network.

https://dx.doi.org/10.21037/qims-2025-1757

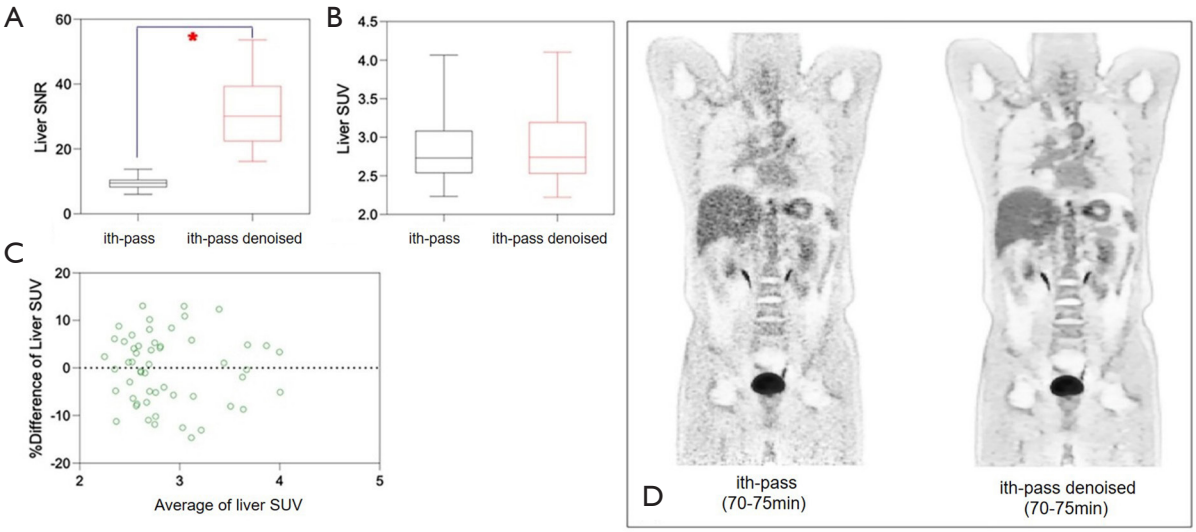

Figure S3 The comparison of liver SNR between each dynamic pass acquired (ith-pass) and its denoised counterpart via the deep learning-based denoising model. (A) The box plot for the liver SNR of the ith-pass (mean SNR 9.5) and that of the corresponding denoised counterpart (mean SNR 31). Paired *t*-tests indicated a significant difference between the ith-pass and its denoised counterpart (P<0.0001). (B) The box plot for the liver SUV for both the acquired ith-pass and its corresponding denoised one. Paired t-tests showed no significant difference between the ith-pass and its denoised counterpart (P=0.35). (C) Bland-Altman plot illustrating the difference between the acquired ith-pass and its corresponding denoised counterpart, with a bias of –0.29 and a bias SD of 7.3 for ith-pass and its-pass after denoising. (D) An example of the coronal SUV image for the acquired ith-pass (between 70 and 75 min) and ith-pass after denoising. Visually, the SNR of the denoised image appears to be obviously improved. SUV, standardized uptake value; SD, standard deviation; SNR, signal-to-noise ratio.

https://dx.doi.org/10.21037/qims-2025-1757